BIOCHEMISTRY
including biophysical chemistry & molecular biology

Article

pubs.acs.org/biochemistry
Terms of Use CC-BY

Binding Hotspots of BAZ2B Bromodomain: Histone Interaction Revealed by Solution NMR Driven Docking

Fleur M. Ferguson,[†] David M. Dias,[†] João P. G. L. M. Rodrigues,[‡] Hans Wienk,[‡] Rolf Boelens,[‡] Alexandre M. J. J. Bonvin,[‡] Chris Abell,[†] and Alessio Ciulli*[,†,§]

[†]Department of Chemistry, University of Cambridge, Lensfield Road, Cambridge, CB2 1EW, U.K.

[‡]Bijvoet Center for Biomolecular Research, Faculty of Science − Chemistry, Utrecht University, Padualaan 8, 3584 CH Utrecht, The Netherlands

[§]College of Life Sciences, Division of Biological Chemistry and Drug Discovery, James Black Centre, University of Dundee, Dow Street, Dundee, DD1 5EH, U.K.

Supporting Information

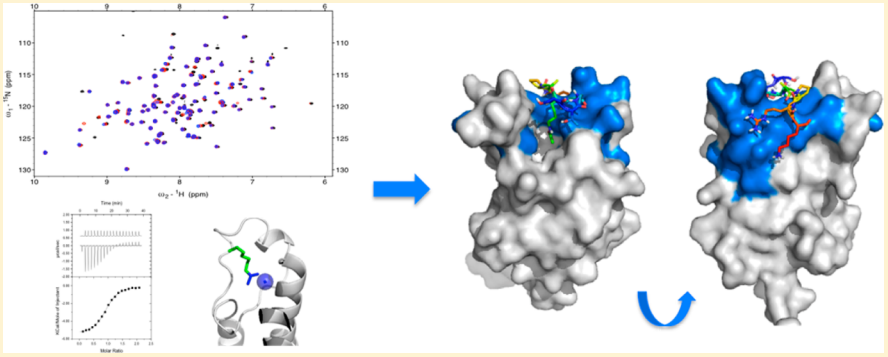

ABSTRACT: Bromodomains are epigenetic reader domains, which have come under increasing scrutiny both from academic and pharmaceutical research groups. Effective targeting of the BAZ2B bromodomain by small molecule inhibitors has been recently reported, but no structural information is yet available on the interaction with its natural binding partner, acetylated histone H3K14ac. We have assigned the BAZ2B bromodomain and studied its interaction with H3K14ac acetylated peptides by NMR spectroscopy using both chemical shift perturbation (CSP) data and clean chemical exchange (CLEANEX-PM) NMR experiments. The latter was used to characterize water molecules known to play an important role in mediating interactions. Besides the anticipated Kac binding site, we consistently found the bromodomain BC loop as hotspots for the interaction. This information was used to create a data-driven model for the complex using HADDOCK. Our findings provide both structure and dynamics characterization that will be useful in the quest for potent and selective inhibitors to probe the function of the BAZ2B bromodomain.

Bromodomains are epigenetic reader domains, which recognize acetylated lysines in a substrate-specific manner.[1] Bromodomain-containing proteins have recently generated much interest from the scientific community due to their roles in transcription, inflammation, and disease.[2] Additionally, generation of potent, selective chemical probes for the BET bromodomains has highlighted this family as tractable targets for small molecule inhibition.[3,4] The BAZ2B protein has an unknown function but is homologous in overall domain organization to the BAZ2A/TIP5 protein,[5] the major subunit of the transcriptional repressor complex NoRC. NoRC establishes a heterochromatic state, preserving genome stability. The complex has also been shown to silence rRNA genes.[6] The BAZ2A and B bromodomains share 57% sequence homology and fall into bromodomain subfamily V.[1]

The BAZ2B bromodomain folds into four helices (αZ, αA, αB, αC), connected by two loops (ZA and BC), forming a typical bromodomain fold.[1] It is known that acetyl lysine binds in a pocket in the center of the four-helix bundle, flanked by the two loops, and that this interaction is mediated by waters occupying the bottom of the pocket (PDB 4NR9[7]), Figure 1.

Previous studies by Philpott et al. based on histone peptide arrays and isothermal titration calorimetry (ITC) characterized histone H3K14ac as the binding partner of the BAZ2B bromodomain.[8] Although a structure of the BAZ2B bromodomain with free acetyl lysine bound is available (PDB 4NR9), how the BAZ2B bromodomain specifically recognizes histone H3 K14ac is still poorly understood as no structural information has yet been reported on a protein−peptide complex.

Received: July 24, 2014
Revised: September 25, 2014
Published: September 30, 2014

 © 2014 American Chemical Society dx.doi.org/10.1021/bi500909d | *Biochemistry* 2014, 53, 6706−6716

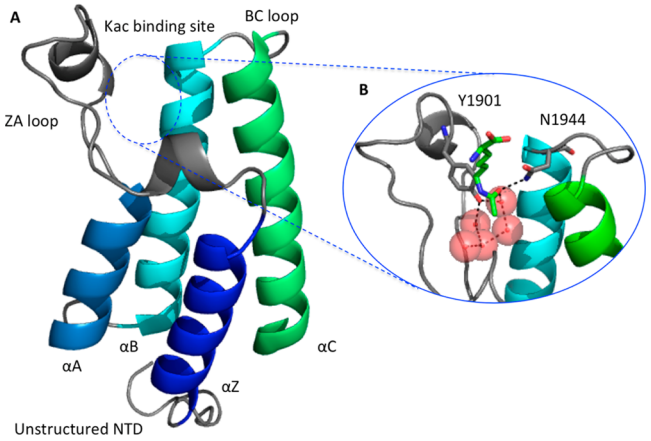

Figure 1. Structural features of the BAZ2B bromodomain. (A) X-ray structure of BAZ2B showing conserved 4-helix fold. (B) Zoom in of binding site occupied by free acetyl lysine and five conserved waters (PDB ID 4NR9).

Acetylated lysine alone is known to interact only very weakly with the BAZ2B bromodomain, but it is necessary for the interaction to occur.[8] We therefore sought to identify and characterize additional interactions contributing to the affinity and specificity of histone H3 Kac14 peptide binding using a combination of biophysical techniques, NMR spectroscopy, and docking simulations. The resulting models were validated with site-directed mutagenesis and peptide binding studies using ITC.

EXPERIMENTAL PROCEDURES

Protein Expression. *Escherichia coli* rosetta competent cells were transformed with a pNIC28 plasmid containing the BAZ2B bromodomain (residues 1868−1972), which has previously been described[1] and used for protein expression. ^{15}N and ^{15}N, ^{13}C- uniformly labeled BAZ2B bromodomains were expressed in M9 medium[9] with 1.5 g of $^{15}NH_4Cl$ (Sigma-Aldrich) and 4.0 g of D-glucose or [U−^{13}C6]-D-glucose (Sigma-Aldrich) per liter as the sole nitrogen and carbon sources. Colonies from freshly transformed cells were grown in 50 mL of M9 medium containing kanamycin (50 μg/mL) at 37 °C with 180 rpm shaking for 16 h. Start up cultures were diluted and inoculated in fresh M9 medium (1 L), containing kanamycin (50 μg/mL), with an initial optical densitiy (OD_{600}) of ∼0.15 and grown at 37 °C with 180 rpm shaking to an optical density (OD_{600}) of ∼0.8. At this point the temperature was decreased to 18 °C, and once the system was equilibrated protein expression was induced with 0.8 mM isopropyl-β-D-thiogalactopyranoside (IPTG) for 18 h. The cells were harvested by centrifugation (6000 rpm, 30 min, 4 °C) using a Beckman Coulter Avanti J-20 XP centrifuge.

Protein Purification. Cell pellets were resuspended in lysis buffer (50 mM HEPES, pH 7.5 at 25 °C, 500 mM NaCl, 5 mM imidazole, 5% glycerol and 0.5 mM TCEP) in the presence of protease inhibitor cocktail and lysed by passing through a French press (three times) at 4 °C. The lysate was cleared by centrifugation at (16000*g*, 1 h, 4 °C) and applied to a HisTrapFF Column (GE Healthcare), equilibrated with lysis buffer. Protein was eluted using a gradient elution of 5−300 mM imidazole. For labeled samples the hexa-histidine-tag was removed by treatment with Tobacco Etch Virus protease (20:1 ratio) in the presence of 0.5 mM EDTA and 1 mM dithiothreitol (DTT) at 4 °C overnight, and protease was removed by running a second HisTrap column. Fractions from chromatography were monitored by SDS-PAGE, using 16% acrylamide gels stained with bromophenol blue. Protein was concentrated and loaded onto Superdex 75 16/60 HiLoad gel filtration column (GE Healthcare) at 4 °C equilibrated with 50 mM HEPES, pH 7.5, 500 mM NaCl, 5% glycerol, 0.5 mM TCEP. Purified protein was concentrated using a Vivaspin-20 concentrator with a 10 000 Da MW cutoff (Vivascience). The absorbance of protein (A_{280}) samples was measured on a Picodrop Microliter UV/vis spectrophotometer (ThermoScientific). Protein concentrations were calculated using molar extinction coefficient predicted using ProtPARAM.[10] The MW of the purified protein was determined using Nanospray-TOF MS, performed on an ABI Q-STAR mass spectrometer. For uniformly ^{15}N labeled BAZ2B bromodomain, the expected MW = 13768 Da, observed MW = 13752, corresponding to 91% incorporation.

Mutagenesis. Site-directed mutagenesis was performed using the QuikChange site-directed mutagenesis kit (Agilent). DNA was purified using a QIAprep Spin kit (Qiagen) following the manufacturer's protocols. Plasmids were sequenced at SourceBiosciences, Cambridge. The absorbance of DNA (A_{260}) samples was measured on a Picodrop Microliter UV/vis spectrophotometer (ThermoScientific). DNA purity was verified by measuring the A_{260}/A_{280} ratio, and all DNA used had $A_{260}/A_{280} > 1.7$.

Differential Scanning Fluorimetry. Thermal Shift experiments were performed using a Lightcycler480 (Roche). Experiments were carried out using 10 μM protein in 50 mM HEPES pH 7.5, 150 mM NaCl, 2.5x SyproOrange (Sigma-Aldrich). Melting temperatures are reported as the average of three measurements.

Isothermal Titration Calorimetry. All experiments were carried out using an ITC200 microcalorimeter (GE Healthcare) at 10 °C, unless otherwise stated, while stirring at 1000 rpm. Experiments were carried out in 50 mM HEPES pH 7.5, 150 mM NaCl. Protein was buffer exchanged using a Pierce protein desalting spin column (Fischer Scientific, UK). All titrations were conducted using an initial injection of 0.4 μL followed by 19 identical injections of 2 μL at a rate of 2 s/μL. Data were corrected for heats of dilution by subtracting the data from independent titrations of ligand into buffer. Data were processed using MicroCal Origin software.

Peptides were either ordered from LifeTein (CellTein) or GenScript, or synthesized using standard Fmoc solid phase peptide synthesis (see Supporting Information). Concentrations were either determined using a Nanodrop spectrophotometer (Thermo Scientific) and the predicted extinction coefficient (ProtPARAM), or by amino acid analysis.

Circular Dichroism Spectroscopy. Proteins were diluted to 0.1 mg/mL in degassed CD buffer (10 mM HEPES, pH 7.4 at 25 °C). CD measurements from a buffer only sample were subtracted from the protein CD measurements. CD experiments were carried out on a Chirascan CD spectrometer (Applied Photophysics) at 25 °C using 0.1 cm quartz cuvettes (Hellma Analytics).

NMR Experiments. $^{15}N/^{13}C$-labeled BAZ2B bromodomain (1 mM) spectra were recorded at 298 K in 20 mM Tris-HCl, pH 7.0 at 25 °C, 100 mM NaCl, 1 mM DTT, and 10% D_2O. Triple resonance, relaxation, small molecule and peptide titration NMR spectra were recorded using a Bruker Avance

dx.doi.org/10.1021/bi500909d | *Biochemistry* 2014, 53, 6706−6716

III 600 spectrometer equipped with a 5 mm TXI $^{1}H-^{13}C/^{15}N/^{2}H$ Z-GRD probe.

BAZ2B bromodomain backbone resonance assignment was performed using 2D [$^{15}N-^{1}H$]-HSQC, and 3D HNCO, HN(CA)CO, CBCA(CO)NH, and HNCACB. These spectra were processed using Bruker Topspin 2.1. Chemical shift perturbations (CSPs) were calculated using the equation:

$$\mathrm{CSP} = \sqrt{\left(\Delta H^2 + \left(\frac{\Delta N}{6.45}\right)^2\right)}$$

In addition, signal intensity changes over the titration were calculated relative to the peak corresponding to the C-terminus (V1971) as an internal reference. A cutoff of 1 standard deviation was used to determine significance of CSPs or intensity changes.

Internal dynamics of BAZ2B bromodomain were obtained using ^{15}N-R1, ^{15}N-R2, and $^{15}N\{^{1}H\}$-heteronuclear NOE relaxation values and were obtained as described previously.[11] ^{15}N-R1 data were obtained from decaying peak intensities in a randomized series of spectra recorded with relaxation delays of 10, 20, 40, 80, 160, 400, 1000, 2000, 4000, 6000, and 7000 ms. R2-values were extracted from CPMG spectra recorded with relaxation delays of 32, 64, 95, 127, 158, 190, 222, and 286 ms. Signal intensities were fitted using Curvefit.[12] Heteronuclear NOEs were obtained using signal intensity ratios from experiments with proton saturation of 5 s and without. For model free analyses, errors in R1 and R2 values were estimated to be 3% of the value, and for heteronuclear NOE an error of 0.05 was assumed. FAST-Modelfree[13] was used to perform the model-free analysis. Chemical shifts, relaxation rates, and heteronuclear NOE values are deposited in BMRB accession number 25105.

Molecular Dynamics. Molecular dynamics calculations were performed using GROMACS v4.5.3.[14] Starting coordinates were obtained from the X-ray crystal structure of apo-BAZ2B (PDB 3G0L) containing a total of 117 residues. Crystal waters further than 5 Å from the Kac binding site were removed. pK_a calculations of residues were carried out using PROPKA3.0 web server[15] to estimate of the protonation states of residues at pH 7.5. No residues were found to have nonstandard protonation states, and the protein is uncharged at this pH; therefore, no ions were added to the simulation water box. The protein was solvated in an octahedral TIP3P water box extending 1 nm from the edge of the protein. Minimization was carried out using a steepest descent algorithm. Particle-Mesh-Ewald (PME) summation was applied to treat long-range interactions, and a cutoff of 0.9 nm was applied for nonbonded interactions. A 0.2 ns equilibration with harmonic restraints was carried out followed by a 225 ns production free MD simulation, performed using the AMBER99SB-STAR-ILDN force field[16] with a time step of 2 fs.

HADDOCK Docking. HADDOCK is a data-driven docking program tailored to model protein interactions using experimental data as restraints. The protein-peptide docking protocol requires specific adaptations to accommodate the higher flexibility of the peptide molecule.[17] The input peptide ensemble consisted of two conformations—extended β-sheet and U-turn–based on an observation of different crystallized bromodomain–peptide complexes. PyMOL was used to build the extended conformation peptide, using −139° for ϕ and −135° for ψ dihedral angles. The U-turn conformation peptide was taken from the NMR structure of the second bromodomain of PB1 bound to H3K14ac histone peptide (PDB ID 2KTB[18]). Unambiguous distance restraints were generated from the Kac-bound crystal structure of BAZ2B (PDB ID 4NR9[7]) to anchor the acetyl group on the lysine side chain in the binding site and restrain the interaction of a conserved water molecule with Y1901. The protein active residues were defined as those whose CSP values or peak intensity decreases are more than 1 σ from the average. The peptide was defined entirely as passive except for the acetyl lysine residue, which was defined as active. All calculations were run through the HADDOCK Web server[19] (http://haddock.science.uu.nl/services/HADDOCK), which implements version 2.1 of the software. Each calculation generated 5000/400/400 models for the different it0/it1/water refinement stages of HADDOCK. The final 400 models were clustered based on their interface-ligand RMSD using a cutoff of 5 Å. The final overall score of each cluster is based on the four highest HADDOCK scores of the models in that cluster.

RESULTS

BAZ2B Bromodomain Resonance Assignments. In order to provide a practical structural tool for mapping ligands in its binding site, we assigned the backbone amide protons of the BAZ2B bromodomain by NMR spectroscopy. These assignments enable high-throughput binding site validation of small molecules or other known interacting partners (~8 min per 2D [$^{15}N-^{1}H$]-HSQC experiment).

The majority of signal intensities in the 2D [$^{15}N-^{1}H$]-HSQC spectrum were assigned unambiguously (89% backbone amide completeness, Figure 2A and Supplementary Table 1). Besides the N-terminus (S1856 to S1867) only D1885 was missing, yielding a total coverage of 99% of the structured protein. The missing D1885 assignment might be due to resonance overlapping. The secondary structure predicted with TALOS + is in overall agreement with the X-ray structure (PDB ID 3G0L) (Figure 2B–C). We observed significant differences in signal intensity for some residues, for instance, D1946. This led us to further investigate the BAZ2B bromodomain internal dynamics using solution NMR.

Internal Dynamics of the BAZ2B Bromodomain. Heteronuclear ^{15}N relaxation R2/R1 ratios (Figure 3) reveal not a completely homogeneous distribution across the structured protein, which can be attributed to either internal dynamics or overall tumbling anisotropy. Overall the values of the heteronuclear NOEs fall predominantly in the range 0.7–0.9, indicating a relatively rigid core. Three residues at the C-terminus (K1970, V1971, and S1972) may undergo fast internal dynamics, as indicated by reduced R2/R1 ratios and [$^{15}N-^{1}H$]-heteronuclear NOE values (Figure 3A,B), suggesting that this region may be unstructured in solution. Consistent with this observation, residues 1971 and 1972 are not visible in X-ray structures of this construct.

The rotational correlation time (τ_c) of a protein is dependent on its size, shape, and dynamics in solution; hence this parameter is used to gauge overall rotational motion information. However, for nonspherical proteins the best assessment of these motions can be modeled using an axially symmetric tensor (characterized by diffusion constants around the unique ($D_{\parallel}$) and perpendicular ($D_{\perp}$) axes). For BAZ2B, the τ_c found was 10.86 ± 0.04 ns, being higher than the value predicted with HYDRONMR[20] (7.5 ns). To rule out the possibility of dimerization or increased viscosity, we performed diffusion-ordered spectroscopy (DOSY[21]), which confirmed

dx.doi.org/10.1021/bi500909d | Biochemistry 2014, 53, 6706–6716

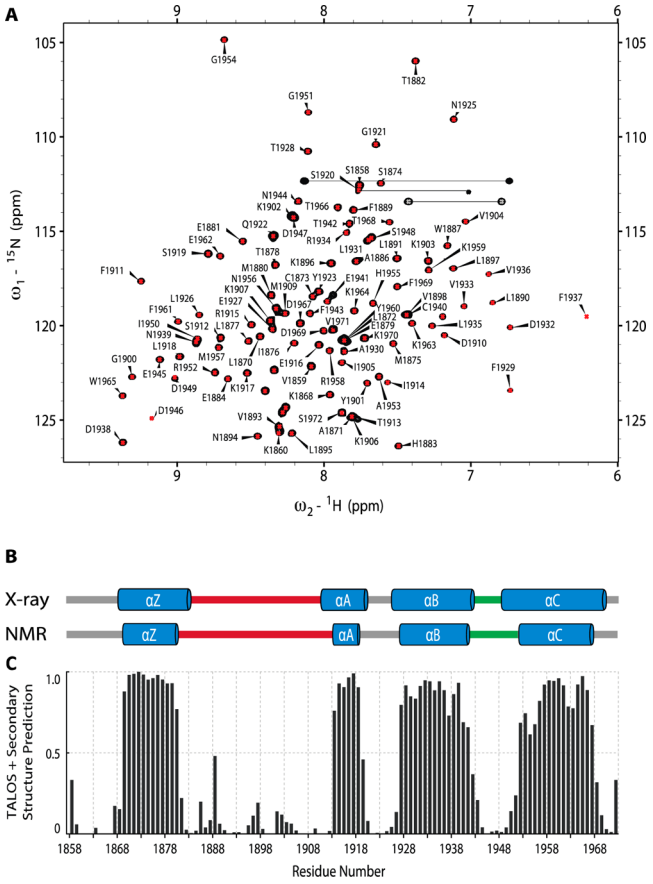

Figure 2. BAZ2B spectral assignment (A) 2D [^{15}N−^{1}H]-HSQC showing the assignment of BAZ2B bromodomain backbone amide peaks. (B) Comparison of the NMR secondary structure prediction to that seen in the X-ray structure of this construct (PDB ID 3G0L). (C) Secondary structure prediction using Talos+ (bars represent α helix propensity).

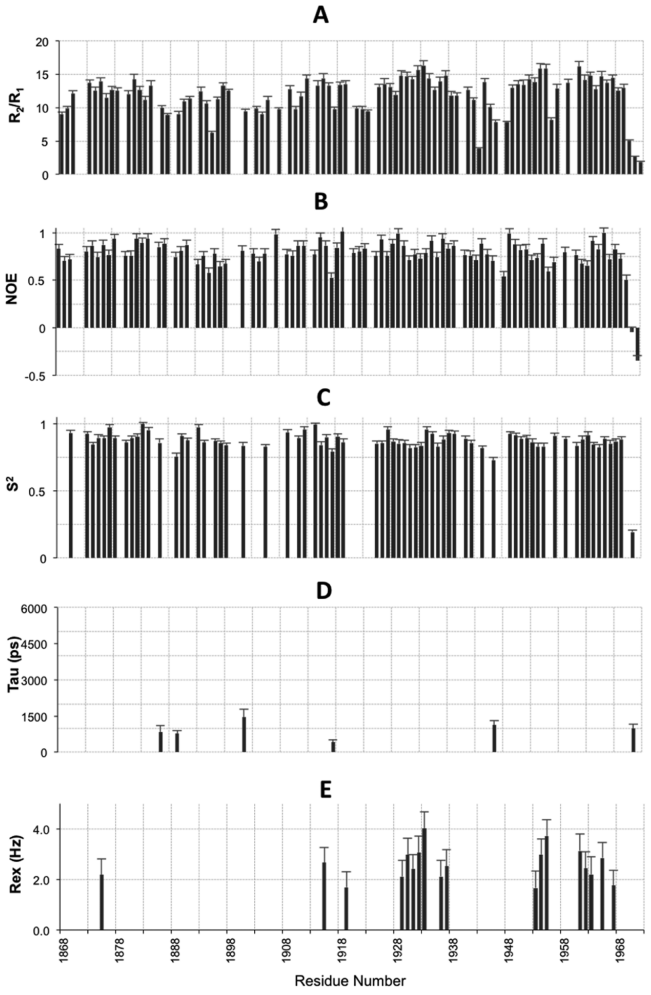

Figure 3. Parameters describing internal dynamics for the assigned and nonoverlapping residues of BAZ2B bromodomain. (A) ^{15}N-R2/R1 ratios; (B) ^{15}N{^{1}H}-heteronuclear NOE values; (C) squared general order parameters, S^2; (D) fast (ns−ps) internal motions expressed as internal correlation times, τ_i (ps); (E) slow (ms−μs) dynamics expressed as exchange contribution to the line shape, R_{ex} (Hz).

the monomeric form of BAZ2B only, since it is diffusing in line with its molecular weight (data not shown). Accordingly the protein elutes as a single peak in size-exclusion chromatography (Supplementary Figure 1, Supporting Information). The slightly increased τ_c value is in agreement with what has been observed for other proteins in this family (BRD4 BD2, 14.8 ns[22]). We suspect the value is higher than predicted because the slightly extended unstructured N-terminal region of the protein (residues S1856−S1867) influences the tumbling in solution. The slight anisotropy of the axial symmetric rotational diffusion tensor ($D_{\parallel}/D_{\perp}$ = 1.14) is consistent with the somewhat elongated shape also found in the X-ray crystal structure (PDB code 3G0L) and explains the trends in observed R1/R2 ratios (Figure 3).

In order to separate the overall tumbling properties of the BAZ2B bromodomain from its internal dynamics, model-free analysis was performed with FAST-Modelfree,[13] using the standard combinations of contributions to internal motions (i.e., (1) squared generalized order parameter S^2, (2) S^2 and internal correlation time τ_i, (3) S^2 and slow conformational exchange term R_{ex}, (4) S^2 and τ_i and R_{ex}, and (5) S^2 and τ_i and extra order parameter for fast internal motions S^2_f). Most of the residues fell in model 1 which indicates high rigidity of the BAZ2B bromodomain in the ps−ns time scale. Few isolated residues show either fast or slow dynamic propensity. Higher values for τ_i, showing fast internal motions (ps−ns), are found in residues in the ZA loop (A1886, F1889, and Y1901) and the BC loop (D1946), along with C-terminal residue V1971 (Figure 3D). These regions depict values of τ_i on the order of 1 ns. Residues with slow exchange contributions (R_{ex}), at around 3 Hz, are located in helices B and C and involve interhelical contacts (F1929 to F1937 on helix B, A1953 to H1955 and F1961 to D1967 on helix C) (Figure 3E).

Molecular Dynamics Simulations. Molecular dynamics simulations were carried out to further assess the internal dynamics of the BAZ2B bromodomain (see Supplementary Figure 2 for RMSD plotted over the simulation). Throughout a 225 ns simulation all four helices remained stable, with the root-mean-square fluctuation (RMSF) of the backbone atoms below 0.1 nm for most residues (Figure 4B). Residues with a high average RMSF over the simulation were clustered mostly at the N-termini (unstructured region) and in the ZA loop, with some additional residues undergoing fast dynamics also detected in the BC loop and the turn joining the A and B helices (Figure 4). This is in agreement with the NMR dynamics analysis. Principle component analysis of the simulation was conducted to examine correlated motions. The first eigenvector of this analysis revealed a movement in

dx.doi.org/10.1021/bi500909d | Biochemistry 2014, 53, 6706−6716

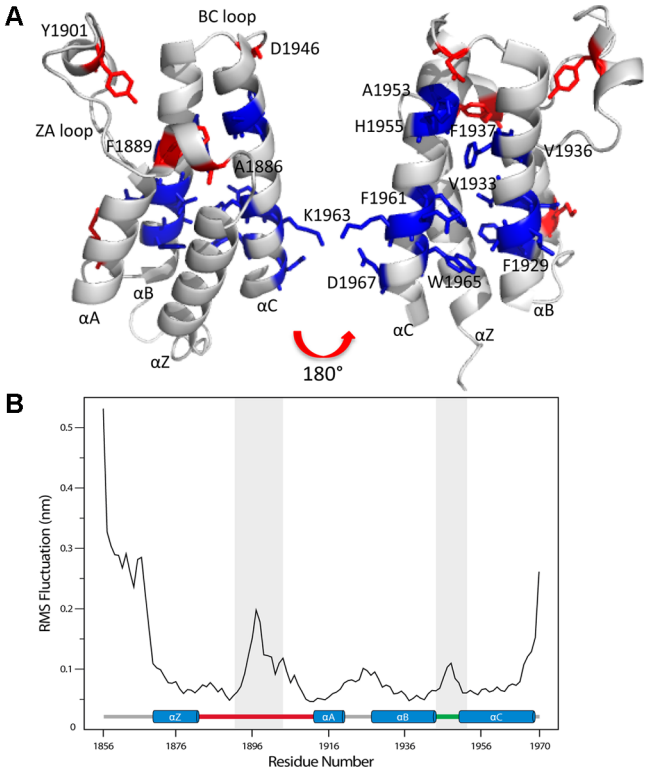

Figure 4. Dynamics of the BAZ2B bromodomain. (A) Experimentally derived dynamics for residues in BAZ2B. Residues with fast (ns−ps) dynamics, shown as red sticks, lie in the ZA and BC loops, or flank these regions. Residues with slow dynamics (μs−ms), shown as blue sticks, reside on the B and C helices. (B) Plot of average RMSF per residue of the BAZ2B bromodomain backbone throughout a 225 ns molecular dynamics simulation. Regions found to display fast internal dynamics by NMR are highlighted in gray.

the upper ZA loop away from the center of the four helix bundle, widening the Kac binding site and reducing its enclosure (Supplementary Figure 3).

Small Molecule HSQC Titration Monitored by [^{15}N−^{1}H]-HSQC. In order to assess the utility of the assigned spectra for mapping ligands to their binding site in the BAZ2B bromodomain, we conducted a titration with Compound 1 (Figure 5B), a reported fragment hit, for which the structure in complex with BAZ2B has been solved using X-ray crystallography (PDB ID 4NRC[7]). Chemical shift perturbations (CSPs) were observed in the BAZ2B [^{15}N−^{1}H]-HSQC spectrum for the peaks of residues in direct contact with the titrated ligand (e.g., F1889, Figure 5B). Additional CSPs were seen in residues close to the fragment binding site (A1953, N1939, L1891), (Figure 5A). Three residues (A1871, M1875, and F1929) at the bottom of the Z and B helices also showed CSPs (shown as gray sticks in Figure 5A). This has also been observed upon titration of peptides into the BRPF1 bromodomain and may be due to small conformational changes in the protein upon ligand binding.[23]

Mapping Histone H3 K14ac Peptide Binding. BAZ2B is reported to bind a 22-mer histone H3 peptide acetylated at lysine 14.[8] As docking programs usually fail to correctly model long, flexible molecules, we synthesized a shorter peptide, Peptide 1, comprised of residues 11−19 of histone H3K14ac. We verified the binding of both peptides to BAZ2B and determined binding constants using ITC. Peptide 1 binds to the BAZ2B bromodomain with a K_D of 45.0 ± 3.3 μM, while the reported Peptide 2 (H3K14ac residues 6−26, +Y-tag) has a slightly higher affinity, 12.2 ± 0.5 μM (Supplementary Table 2), consistent with the previously reported value.[8]

Interacting residues were characterized by measuring 2D [^{15}N−^{1}H] HSQC spectra of the peptides in complex with labeled BAZ2B bromodomain (Supplementary Figure 4). Multiple concentration dependent effects were observed in the protein spectra upon peptide titration, namely, chemical shift perturbation (CSP, typical for fast exchange) and peaks decreasing in intensity and peaks appearing in the spectra (typical for slow exchange), indicative of an intermediate exchange regime. CSPs and changes in peak intensity were analyzed as described in the Experimental Procedures. Both peptides showed binding to the same region of the protein, yet few additional residues were affected by titration with Peptide 2 compared to Peptide 1, despite it being significantly longer (Figure 6B,C). This observation suggests that both peptides bind with a similar binding mode. More importantly the additional N- and C-terminal residues on the Peptide 2 seem to make few specific contacts with the protein, suggesting that the key binding interactions are encapsulated by Peptide 1 alone, consistent with the relatively small difference in binding affinity between the two peptides.

CLEANEX-PM Experiments. It is known that the BAZ2B bromodomain contains an important network of structural water molecules buried in the Kac binding site. These waters mediate the interaction with Kac and small molecules (Figure

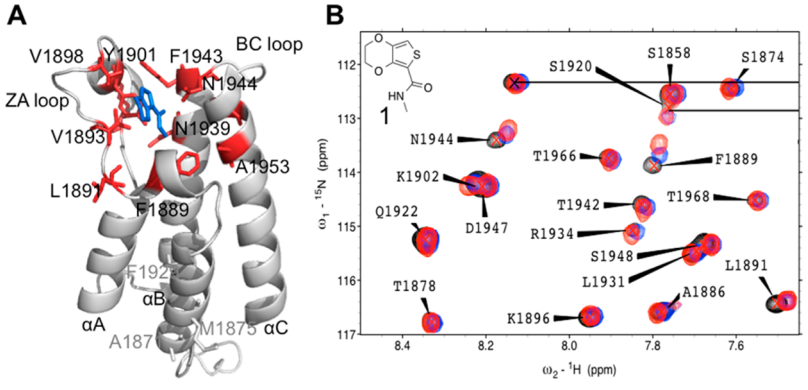

Figure 5. Small molecule HSQC titration. (A) Residues showing significant CSPs upon titration of Compound 1 shown as sticks on X-ray structure (PBD 4NRC),[7] those in the binding site shown in magenta, others shown in gray. (B) Region of the 2D [^{15}N−^{1}H]-HSQC spectra of BAZ2B bromodomain alone (black), with 1 mM Compound 1 (cyan) and 2 mM Compound 1 (magenta). Structure of Compound 1 shown in inset.

dx.doi.org/10.1021/bi500909d | Biochemistry 2014, 53, 6706−6716

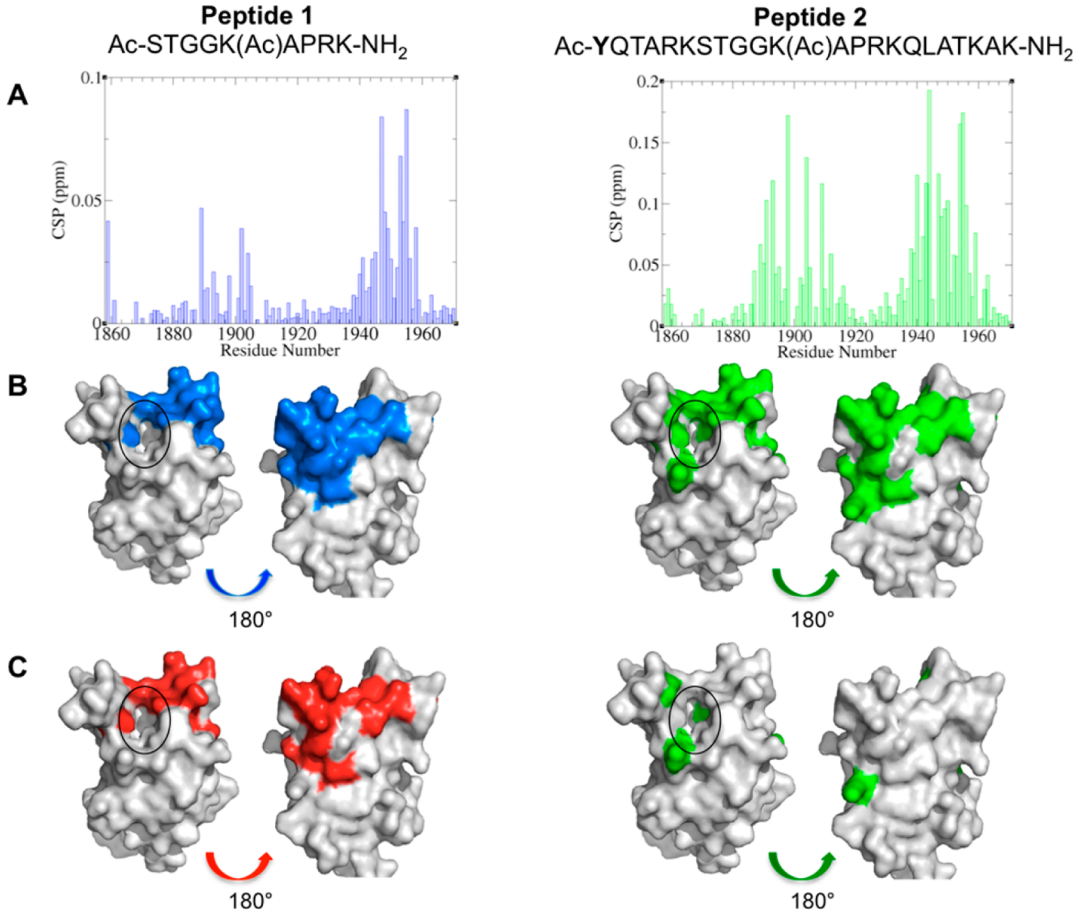

Figure 6. Peptide HSQC titration. (A) Plot of chemical shift perturbations observed upon titration of Peptide 1 or 2 (1:1.2 molar ratio, fractional occupancy 0.93 and 0.84, respectively). (B) Residues affected by peptide titration mapped onto the apo protein surface. (C) Residues shifting in both experiments mapped onto the protein surface, colored red. Residues that show shifts in the Peptide 2 titration but not in the peptide 1 titration are colored green. Kac binding site is highlighted with a circle.

1B) and are conserved.[1] Accordingly they should exchange slowly with the bulk water on the NMR time scale, making them difficult to detect. However, recent simulations by Huang et al.[24] indicate that some of these waters are less tightly bound in the BAZ2B bromodomain and may be able to exchange more rapidly with the bulk solvent and be displaced by a second postulated Kac binding mode.[25] Waters in neighboring regions of the protein should also be detectable. Observing their displacement upon ligand binding may give insight into ligand binding scenarios. It is challenging to obtain bound water signals by NMR directly, and therefore we used an indirect method, Phase-Modulated CLEAN chemical EXchange (CLEANEX-PM) experiment[26] to identify amide protons chemically exchanging with water. In order to examine the change in solvation in the apo and holo forms of BAZ2B, we performed measurements in the presence and absence of Peptide 1.

In both spectra the residues at the N- and C-termini have proton exchange contributions (Figure 7) verifying the possible lack of structured elements in these regions in solution.

The backbone amide of conserved Kac binding site residue Y1901 (Figure 1B) stops exchanging with water upon addition of Peptide 1. A side chain amide resonance also disappears. Comparison of the X-ray crystal structures of apo (PDB 3G0L) and Kac bound (PDB 4NR9[7]) BAZ2B bromodomain shows that the carbonyl oxygen of Kac displaces water bound to N1944 side chain from the binding site (Figure 1B), consistent with this CLEANEX-PM result. No peaks are detectable for residues at the base of the Kac binding site, where the conserved structural waters reside, indicating that these waters do not exchange on the time scale of the experiment.

Interestingly backbone amides in the BC loop (E1945, D1946, D1947) stop exchanging with water once the H3 peptide is bound (Figure 7). This may be due to either displacement of waters by the peptide or by the peptide forming stable water-mediated interactions that significantly reduce exchange rates (e.g., H-bond formation). Taken together the CSPs and CLEANEX-PM data indicate the Kac binding site and BC loop as hotspots for binding to the histone H3 tail.

Modeling the Complex Using HADDOCK. The structure of the BAZ2B−Peptide 1 complex was modeled using HADDOCK.[27] Experimental data from our NMR HSQC titrations, and the geometry of acetyl lysine and conserved waters mediating the interaction in the binding site from X-ray crystallography were used to generate distance restraints to drive the docking simulation (see Experimental Procedures). The protein-peptide docking protocol requires specific modifications to accommodate the higher flexibility of the peptide molecule. Therefore, we made minor adaptations to the protocol described by Trellet et al.,[17] based on observations of different crystallized bromodomain−peptide complexes.

dx.doi.org/10.1021/bi500909d | *Biochemistry* 2014, 53, 6706−6716

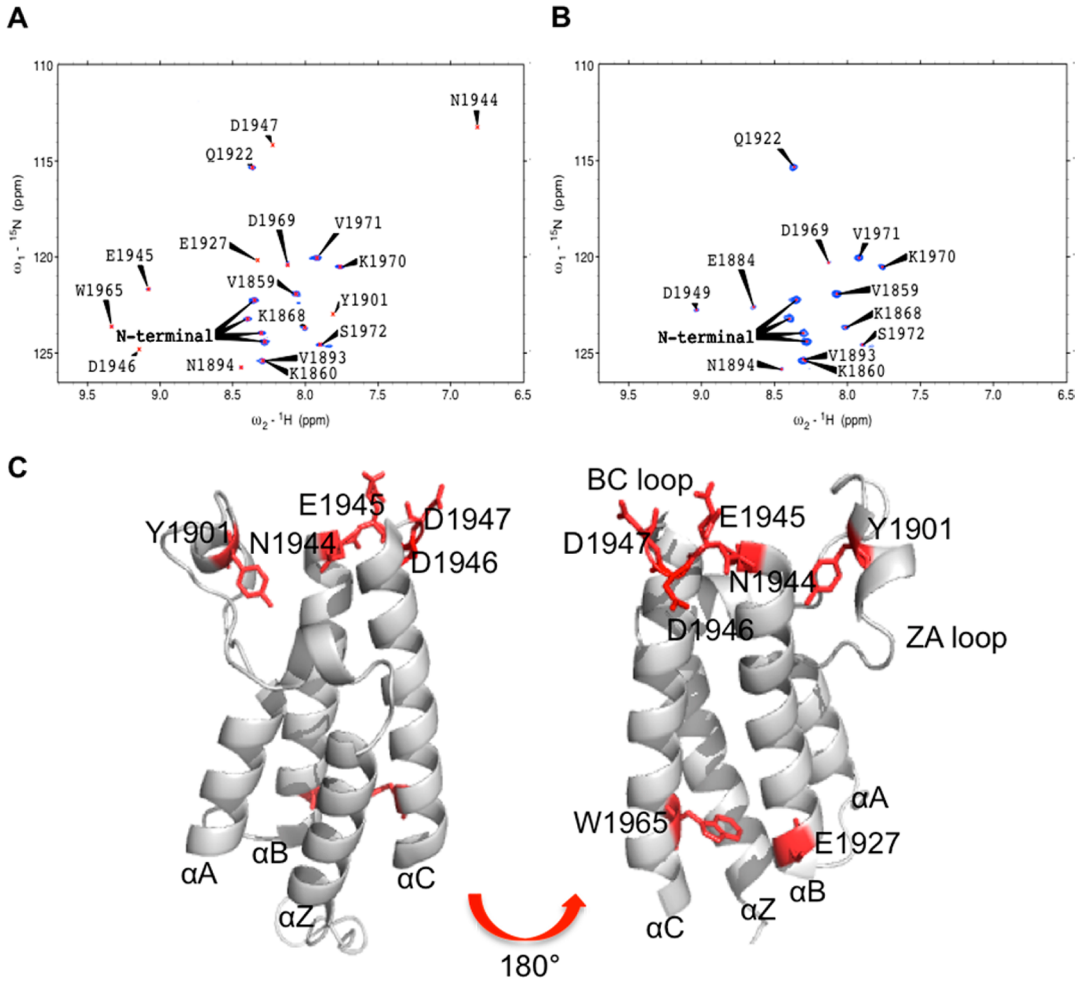

Figure 7. CLEANEX-PM spectra of BAZ2B bromodomain (A) alone and (B) in the presence of Peptide 1. (C) Residues for which signals in the CLEANEX experiment disappear upon addition of Peptide 1, shown as red sticks.

Namely, the input ensemble consisted of the peptide in two conformations—extended β-sheet and U-turn. Alpha helix and Polypro conformations were excluded as preliminary runs showed that no complex structures derived from these progressed through to IT1, and the H3 histone tail has not been reported to adopt either conformation. After docking and water refinement, the four highest scored structures from the top four clusters were analyzed (Figure 8, for the cluster statistics of the run, see Supplementary Table 3).

All models generated place the C-termini of the peptide between the αA and αB helices. The basic residues R17 or K18 are positioned such that they interact with the acidic residues (E1945 and D1946) from the BC loop and the peptide lies in the groove between the ZA loop and the αB-helix. The four top scoring clusters show diverse arrangements for the N-terminal portion of the peptide (residues 10−13), with different models placing it close to the ZA loop, the BC loop, and oriented away from the protein toward the solvent (Figure 8A). This indicates this region of the peptide may not form any specific anchoring interactions with the bromodomain.

Besides the visual examination of individual models, the averaged per-residue interaction energies of the protein and peptide over the ensemble of docked structures were plotted (Figure 8B). Residues with the largest interaction energies in the peptide were K14ac, R17, and K18. Although R17 and K18 have a larger contribution to binding than K14ac in the scoring, it is known that nonacetylated H3 does not interact with the BAZ2B bromodomain.[1] Residues making favorable interactions in the protein are those in the Kac binding site (e.g., residues 1941−1944) and in and close to the BC loop (residues 1945−1949), consistent with the input CSP data.

Model Validation. In order to validate the docking predictions and gain further insight into the structural determinants of the molecular recognition, residues surrounding the Kac binding pocket were mutated. Folding and stability were verified for the mutants using CD spectroscopy and thermal melting experiments (Table 1). Mutations were well tolerated at most sites, minimal changes in helicity observed indicate that the mutant proteins are correctly folded. The protein melting temperature (T_m) was only affected significantly for mutation W1887F, whose melting temperature nevertheless remained above 45 °C.

ITC was used to test which mutations were able to perturb the interaction between the BAZ2B bromodomain and Peptide 2 (Table 1 and Supplementary Table 4). As expected, mutation of V1893 or I1950 to alanine, which are in close proximity to the acetylated lysine, caused a significant 6-fold reduction in binding. Mutation of F1943 had the largest effect on binding. When mutated to a more hydrophobic and bulky leucine residue the affinity was significantly weakened, and after mutation to alanine binding was no longer detectable, indicating that this phenylalanine may be involved in the

dx.doi.org/10.1021/bi500909d | *Biochemistry* 2014, 53, 6706−6716

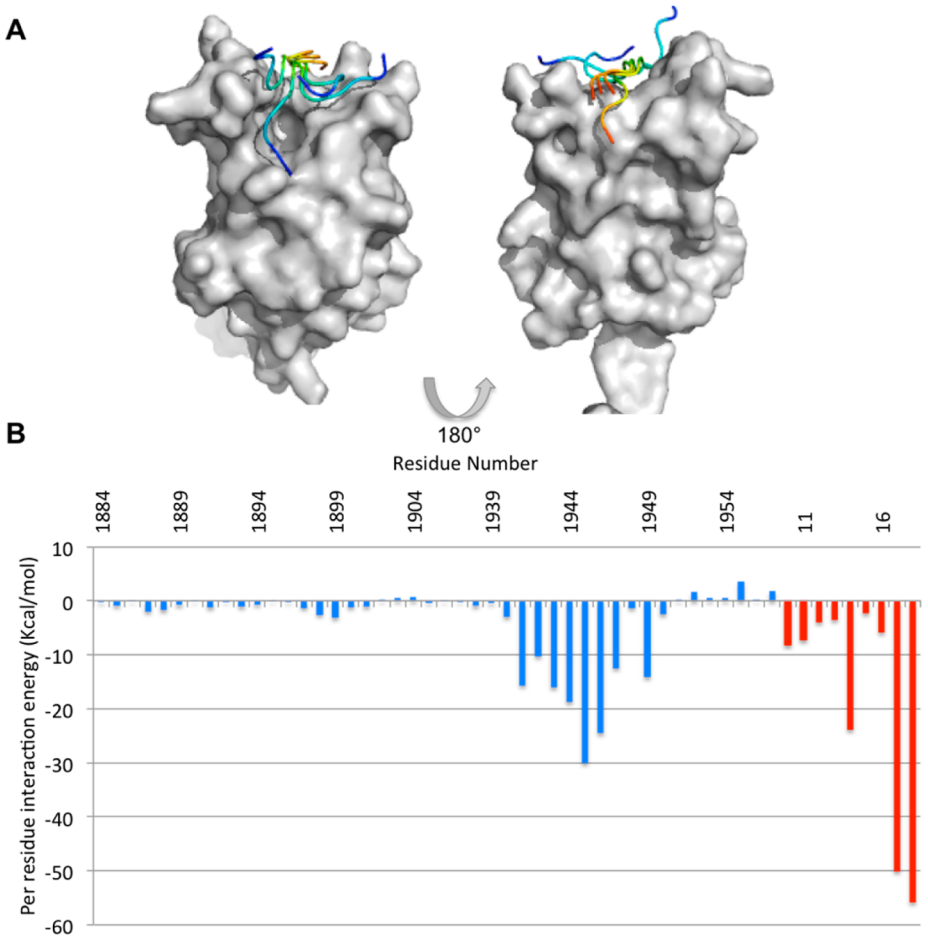

Figure 8. Results of HADDOCK docking (A) Overlay of the top scored models from the top four clusters. (B) Per residue interaction energy (sum of van der Waals and electrostatic energies) for interacting residues in the protein (blue) and peptide (red). Values are shown as an average over the ensemble of output HADDOCK poses.

interaction or may stabilize the required local pocket structure. This is consistent with docked structures placing the peptide in the groove between the B-helix and ZA loop. Mutation of W1887 to alanine in the ZA loop did not affect the binding interaction, consistent with NMR titrations, and in support of HADDOCK models that do not place the peptide in this region. Interestingly mutation of V1898 to alanine also did not affect binding despite NMR CSP data indicating an interaction with Peptide 2 but not Peptide 1 (Figure 6A). Therefore, we propose that contacts may be present between the H3 peptide and this valine side chain, but these interactions are not contributing significantly to the binding affinity.

Peptide Binding. The HADDOCK docking results proposed highly scoring models in which either the peptide's residue K18 (e.g., cluster 1, model 1) or R17 (e.g., cluster 1, model 2) make key interactions with BC loop residues. These residues make similar and significant contributions to the predicted binding energy over the ensemble (Figure 8B). In order to distinguish the importance of these residues, the affinities of a number of H3K14ac peptides of varying length (Peptides 1−7) were measured using ITC (Table 2 and Supplementary Table 5).

Peptide 2 and Peptide 3 have very similar K_D's, indicating that no interaction occurs between BAZ2B and H3 residues more than five amino acids away from K14ac. Removal of Q19 (Peptide 4) has little consequence on binding affinity. Removal of either K9 or K18 (Peptides 1 and 6) led to a 2-fold reduction in affinity relative to Peptide 4. This relatively small effect is not additive, as Peptide 5, where both K9 and K18 are not present, has a similar K_D. This implies K18 is not a key driver of the additional affinity of H3K14ac for BAZ2B. No heats were observed upon titration of 2.4 mM Peptide 7 into 100 μM BAZ2B bromodomain, indicating that the K_D is >2 mM. These results identify R17 as a key determinant of binding and validate HADDOCK models in which R17 makes a large contribution to the binding interactions (Figure 9).

■ DISCUSSION

We have assigned the backbone resonances in the BAZ2B bromodomain $^{15}N-^{1}H$ HSQC spectra and characterized the protein dynamics using NMR spectroscopy and molecular dynamics simulations, revealing a relatively rigid bromodomain in solution. CSPs mapping was validated by titration of a small molecule ligands for which the binding mode has been independently verified. These assignments therefore also provide a useful platform for screening and binding site elucidation of small molecules. In order to provide new chemical tools to uncover the biological role of the BAZ2B bromodomain, a number of compounds have been developed to inhibit its interaction with histones.[7,28] Thus far, ligands predominantly target the small Kac binding site. Identification of additional binding hotspots provides new insights that may

dx.doi.org/10.1021/bi500909d | *Biochemistry* 2014, 53, 6706−6716

Table 1. Melting Temperatures of Wildtype and Point Mutants of BAZ2B Bromodomain As Average of Three Replicates[a]

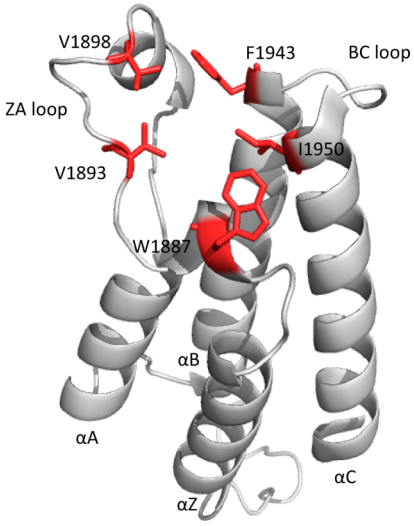

protein	T_m (°C)	ΔT_m vs WT	% α-helix	K_D (μM)
F1943A	53.3	1.0	60	
WT	52.3	0.0	60	12.2 ± 0.5
I1950A	52.2	−0.1	57	64.0 ± 4.1
V1893A	51.3	−1.0	57	66.6 ± 3.7
V1898A	51.3	−1.0	57	9.1 ± 1.0
F1943L	50.2	−2.1	60	127.7 ± 7.8
W1887H	49.3	−3.0	61	16.8 ± 1.2
W1887F	45.2	−7.1	60	10.6 ± 0.2

[a]No variation in T_m was observed between replicates. % α-Helix from CD measurements calculated according to Corrêa et al.[32] Binding affinities of BAZ2B bromodomain mutants for Peptide 2 measured using ITC.

aid future efforts to generate novel selective chemical probes for this bromodomain.

Interestingly we observed an intermediate exchange regime for two H3K14ac peptides, although one of their K_D's falls within a range that should be under a fast exchange regime (Peptide 1, 45.0 ± 3.3 μM). The relatively different contributions to affinity of peptide residues may explain peaks appearing/disappearing; e.g., the BC loop residues D1945 and E1946 consistently show significantly reduced intensity in both titrations. Interestingly the BAZ2 bromodomains are the only ones in the family to contain three sequential acidic residues in their BC loop,[1] and we observed that this patch is indeed involved in the interaction. The data consistently highlight the BC loop as a key hotspot for interaction with H3 peptides, in addition to the Kac binding site. Residue R17 on histone H3 was found to be the crucial

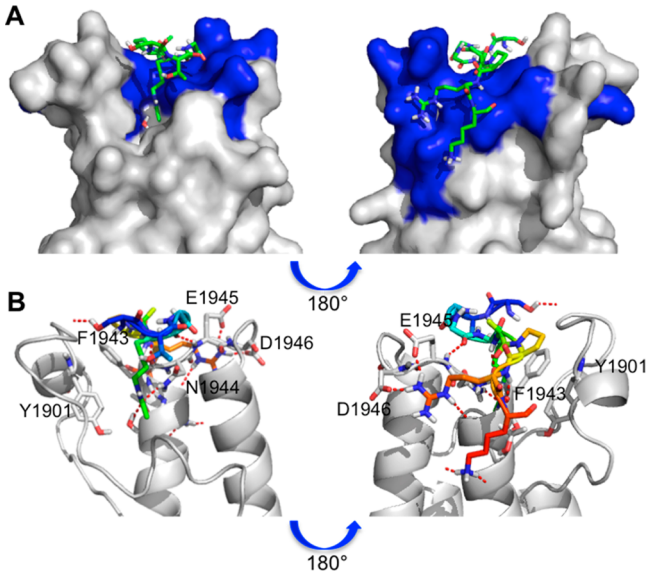

Figure 9. (A) Surface view of the HADDOCK model of the BAZ2B/Peptide 1 complex in closest agreement with experimental data. Residues with CSPs upon titration of Peptide 1 are colored blue. (B) Alternate view of the HADDOCK model, BAZ2B shown gray, interacting residues shown as sticks, H-bonds shown as red dashed lines.

additional interacting residue of H3, conferring affinity to the interaction. Mutagenesis data also highlighted F1943 as an important residue for binding.

Water molecules play an important role in bromodomain−ligand interactions. For the first time we have monitored changes in water exchange rates upon peptide binding in a bromodomain using CLEANEX-PM experiments, in a qualitative manner. These experiments re-enforced the involvement of the BC loop in H3 peptide recognition consistent with the binding mode of the modeled peptide.

There has been much recent interest in the water molecules at the bottom of the bromodomain Kac binding pocket from a drug design standpoint.[24,25] Key questions are to what extent they are displaceable and whether a small molecule should be designed to hydrogen bond to them or to displace them and form the same interactions as the waters do.[24,29] Thus far, this question has only been addressed using MD simulations. Extension of the CLEANEX-PM experiments to observe different exchange rates may provide additional insight into which waters in this pocket are stable and how this differs between different bromodomains.

In conclusion, the key determinants for the BAZ2B/H3K14ac peptide interaction have been elucidated using a combination of biophysical and computational techniques. Such an approach allowed us to characterize both protein and

Table 2. Binding Affinities of H3K14ac Peptides for BAZ2B Bromodomain

peptide no.	peptide sequence	K_D (μM)
1	Ac-STGGK(ac)APRK-NH_2	45.0 ± 3.3
2	Ac-YQTARKSTGGK(Ac)APRKQLATKAK-NH_2	12.2 ± 0.5
3	Ac-KSTGGK(ac)APRKQ-NH_2	15.7 ± 1.1
4	Ac-KSTGGK(ac)APRK-NH_2	21.8 ± 1.4
5	Ac-STGGK(ac)APR-NH_2	52.4 ± 2.4
6	Ac-KSTGGK(ac)APR-NH_2	37.6 ± 2.1
7	Ac-KSTGGK(ac)AP-NH_2	>2000

dx.doi.org/10.1021/bi500909d | *Biochemistry* 2014, 53, 6706−6716

peptide contributions and provide structural insights into the molecular recognition. This strategy is generally applicable to many bromodomain−peptide interactions and provides a convenient alternative to structure determination by NOE-based NMR or X-ray crystallography in challenging cases where the acetylated interacting partner has a relatively weak affinity (high micromolar to millimolar) for the bromodomain, as is the case for many of the reported histone−bromodomain interactions[30] for which there are no currently available structures (e.g., BRD7:H3K14ac, K_D 1.9 mM[31]).

■ ASSOCIATED CONTENT

Supporting Information

Peptide synthesis procedures, Supplementary Figures 1−4, and Supplementary Tables 1−5. This material is available free of charge via the Internet at http://pubs.acs.org.

■ AUTHOR INFORMATION

Corresponding Author

*E-mail: a.ciulli@dundee.ac.uk. Phone: +44 1382 386230. Fax: +44 1382 386373.

Funding

This work was supported by the UK Biotechnology and Biological Sciences Research Council (BBSRC, Grants BB/J001201/1 and David Phillips Fellowship BB/G023123/1 to A.C.). F.M.F. is funded by a BBSRC Ph.D studentship. D.M.D. acknowledges the Fundação para a Ciência e a Tecnologia (FCT, SFRH/BD/81735/2011 Studentship). J.P.G.L.M. and A.M.J.J.B. acknowledge the financial support from Utrecht University (Focus and Massa Programme) and The Netherlands Organization for Scientific Research (VICI Grant No. 700.56.442). Financial support by the European Union (BioNMR, Project 261863) for access to the SONNMR Large-Scale Facility in Utrecht (The Netherlands) is gratefully acknowledged.

Notes

The authors declare no competing financial interest.

■ ACKNOWLEDGMENTS

The authors would like to thank Stefan Knapp at SGC Oxford for the BAZ2B bromodomain plasmid.

■ ABBREVIATIONS

BAZ2A, bromodomain adjacent to zinc finger domain protein 2A; BAZ2B, bromodomain adjacent to zinc finger domain protein 2B; BET, bromodomain and extraterminal domain; BRPF1, bromodomain and PHD finger containing protein 1; CD, circular dichroism; CLEANEX-PM, phase modulated CLEAN chemical EXchange; CSP, chemical shift perturbation; DOSY, diffusion-ordered spectroscopy; H3K14ac, histone H3 acetylated at lysine 14; HADDOCK, high ambiguity data-driven docking; HSQC, heteronuclear single quantum correlation; ITC, isothermal titration calorimetry; Kac, *N*-ε-acetyl lysine; NoRC, nucleolar remodeling complex; NOE, Nuclear Overhauser effect; RMSD, root-mean-square deviation; RMSF, root-mean-square fluctuation; rRNA, ribosomal ribonucleic acid; T_m, thermal melting temperature

■ REFERENCES

(1) Filippakopoulos, P., Picaud, S., Mangos, M., Keates, T., Lambert, J.-P., Barsyte-Lovejoy, D., Felletar, I., Volkmer, R., Müller, S., Pawson, T., Gingras, A.-C., Arrowsmith, C. H., and Knapp, S. (2012) Histone Recognition and Large-Scale Structural Analysis of the Human Bromodomain Family. *Cell 149* (1), 214−231.

(2) Muller, S., Filippakopoulos, P., and Knapp, S. (2011) Bromodomains as therapeutic targets. *Expert Rev. Mol. Med. 13*, e29.

(3) Nicodeme, E., Jeffrey, K. L., Schaefer, U., Beinke, S., Dewell, S., Chung, C.-w., Chandwani, R., Marazzi, I., Wilson, P., Coste, H., White, J., Kirilovsky, J., Rice, C. M., Lora, J. M., Prinjha, R. K., Lee, K., and Tarakhovsky, A. (2010) Suppression of inflammation by a synthetic histone mimic. *Nature 468* (7327), 1119−1123.

(4) Filippakopoulos, P., Qi, J., Picaud, S., Shen, Y., Smith, W. B., Fedorov, O., Morse, E. M., Keates, T., Hickman, T. T., Felletar, I., Philpott, M., Munro, S., McKeown, M. R., Wang, Y., Christie, A. L., West, N., Cameron, M. J., Schwartz, B., Heightman, T. D., La Thangue, N., French, C. A., Wiest, O., Kung, A. L., Knapp, S., and Bradner, J. E. (2010) Selective inhibition of BET bromodomains. *Nature 468* (7327), 1067−1073.

(5) Jones, M. H., Hamana, N., Nezu, J., and Shimane, M. (2000) A novel family of bromodomain genes. *Genomics 63* (1), 40−45.

(6) Guetg, C., Lienemann, P., Sirri, V., Grummt, I., Hernandez-Verdun, D., Hottiger, M. O., Fussenegger, M., and Santoro, R. (2010) The NoRC complex mediates the heterochromatin formation and stability of silent rRNA genes and centromeric repeats. *EMBO J. 29* (13), 2135−2146.

(7) Ferguson, F. M., Fedorov, O., Chaikuad, A., Philpott, M., Muniz, J. R. C., Felletar, I., von Delft, F., Heightman, T., Knapp, S., Abell, C., and Ciulli, A. (2013) Targeting Low-Druggability Bromodomains: Fragment Based Screening and Inhibitor Design against the BAZ2B Bromodomain. *J. Med. Chem. 56* (24), 10183−10187.

(8) Philpott, M., Yang, J., Tumber, T., Fedorov, O., Uttarkar, S., Filippakopoulos, P., Picaud, S., Keates, T., Felletar, I., Ciulli, A., Knapp, S., and Heightman, T. D. (2011) Bromodomain-peptide displacement assays for interactome mapping and inhibitor discovery. *Mol. BioSystems 7* (10), 2899−2908.

(9) Marley, J., Lu, M., and Bracken, C. (2001) A method for efficient isotopic labeling of recombinant proteins. *J. Biomol. NMR 20* (1), 71−75.

(10) Artimo, P., Jonnalagedda, M., Arnold, K., Baratin, D., Csardi, G., de Castro, E., Duvaud, S., Flegel, V., Fortier, A., Gasteiger, E., Grosdidier, A., Hernandez, C., Ioannidis, V., Kuznetsov, D., Liechti, R., Moretti, S., Mostaguir, K., Redaschi, N., Rossier, G., Xenarios, I., and Stockinger, H. (2012) ExPASy: SIB bioinformatics resource portal. *Nucleic Acids Res. 40(W1)*, W597−W603.

(11) Wienk, H., Tishchenko, E., Belardinelli, R., Tomaselli, S., Dongre, R., Spurio, R., Folkers, G. E., Gualerzi, C. O., and Boelens, R. (2012) Structural dynamics of bacterial translation initiation factor IF2. *J. Biol. Chem. 287* (14), 10922−32.

(12) Curvefit Homepage. http://www.palmer.hs.columbia.edu/software/curvefit.html (accessed 21/04/2014).

(13) Cole, R., and Loria, J. P. (2003) FAST-Modelfree: A program for rapid automated analysis of solution NMR spin-relaxation data. *J. Biomol. NMR 26* (3), 203−213.

(14) Hess, B., Kutzner, C., van der Spoel, D., and Lindahl, E. (2008) GROMACS 4: Algorithms for Highly Efficient, Load-Balanced, and Scalable Molecular Simulation. *J. Chem. Theory Comput. 4* (3), 435−447.

(15) Olsson, M. H. M., Søndergaard, C. R., Rostkowski, M., and Jensen, J. H. (2011) PROPKA3: Consistent Treatment of Internal and Surface Residues in Empirical pK_a Predictions. *J. Chem. Theory Comput. 7* (2), 525−537.

(16) Best, R. B., de Sancho, D., and Mittal, J. (2012) Residue-Specific α-Helix Propensities from Molecular Simulation. *Biophys. J. 102* (6), 1462−1467.

(17) Trellet, M., Melquiond, A. S. J., and Bonvin, A. M. J. J. (2013) A Unified Conformational Selection and Induced Fit Approach to Protein-Peptide Docking. *PLoS One 8* (3), e58769.

(18) Charlop-Powers, Z., Zeng, L., Zhang, Q., and Zhou, M.-M. (2010) Structural insights into selective histone H3 recognition by the human Polybromo bromodomain 2. *Cell Res. 20* (5), 529−538.

(19) de Vries, S. J., van Dijk, M., and Bonvin, A. M. J. J. (2010) The HADDOCK web server for data-driven biomolecular docking. *Nat. Protocols 5* (5), 883−897.
(20) García de la Torre, J., Huertas, M. L., and Carrasco, B. (2000) HYDRONMR: Prediction of NMR Relaxation of Globular Proteins from Atomic-Level Structures and Hydrodynamic Calculations. *J. Magn. Reson. 147* (1), 138−146.
(21) Morris, K. F., and Johnson, C. S. (1992) Diffusion-ordered two-dimensional nuclear magnetic resonance spectroscopy. *J. Am. Chem. Soc. 114* (8), 3139−3141.
(22) Liu, Y., Wang, X., Zhang, J., Huang, H., Ding, B., Wu, J., and Shi, Y. (2008) Structural Basis and Binding Properties of the Second Bromodomain of Brd4 with Acetylated Histone Tails. *Biochemistry 47* (24), 6403−6417.
(23) Poplawski, A., Hu, K., Lee, W., Natesan, S., Peng, D., Carlson, S., Shi, X., Balaz, S., Markley, J. L., and Glass, K. C. (2014) Molecular Insights into the Recognition of N-Terminal Histone Modifications by the BRPF1 Bromodomain. *J. Mol. Biol. 426* (8), 1661−1676.
(24) Huang, D., Rossini, E., Steiner, S., and Caflisch, A. (2013) Structured Water Molecules in the Binding Site of Bromodomains Can Be Displaced by Cosolvent. *ChemMedChem*, 573−579.
(25) Magno, A., Steiner, S., and Caflisch, A. (2013) Mechanism and kinetics of acetyl-lysine binding to bromodomains. *J. Chem. Theory Comput. 9* (9), 4225−4232.
(26) Hwang, T.-L., van Zijl, P. M., and Mori, S. (1998) Accurate Quantitation of Water-amide Proton Exchange Rates Using the Phase-Modulated CLEAN Chemical EXchange (CLEANEX-PM) Approach with a Fast-HSQC (FHSQC) Detection Scheme. *J. Biomol. NMR 11* (2), 221−226.
(27) Dominguez, C., Boelens, R., and Bonvin, A. M. J. J. (2003) HADDOCK: A Protein−Protein Docking Approach Based on Biochemical or Biophysical Information. *J. Am. Chem. Soc. 125* (7), 1731−1737.
(28) GSK2801: A Selective Chemical Probe for BAZ2B/A bromodomains. http://www.thesgc.org/scientists/chemical_probes/GSK2801 (accessed 05/08/2013).
(29) Fedorov, O., Lingard, H., Wells, C., Monteiro, O. P., Picaud, S., Keates, T., Yapp, C., Philpott, M., Martin, S. J., Felletar, I., Marsden, B. D., Filippakopoulos, P., Müller, S., Knapp, S., and Brennan, P. E. (2013) [1,2,4]Triazolo[4,3-a]phthalazines: Inhibitors of Diverse Bromodomains. *J. Med. Chem. 57* (2), 462−476.
(30) Filippakopoulos, P., and Knapp, S. (2012) The bromodomain interaction module. *FEBS Lett. 586* (17), 2692−2704.
(31) Sun, H., Liu, J., Zhang, J., Shen, W., Huang, H., Xu, C., Dai, H., Wu, J., and Shi, Y. (2007) Solution structure of BRD7 bromodomain and its interaction with acetylated peptides from histone H3 and H4. *Biochem. Biophys. Res. Commun. 358* (2), 435−441.
(32) Corrêa, D. H., and Ramos, C. H. (2009) The use of circular dichroism spectroscopy to study protein folding, form and function. *Afr. J. Biochem Res. 3* (5), 164−173.